In: Tolxdorff, T., Braun, J., Handels, H., Horsch, A., Meinzer, H.-P. (Hrsg.): Bildverarbeitung für die Medizin 2004 - Algorithmen, Systeme, Anwendungen (Tagungsband zum Workshop BVM'2004, Erlangen), Reihe Informatik aktuell im Springer-Verlag, S. 70-74, März 2004

Quantification of Tumour Invasion Fronts using 3D Reconstructed Histological Serial Sections

Ulf-Dietrich Braumann[1], Jens-Peer Kuska[2], Jens Einenkel[3], Lars-Christian Horn[4], and Michael Höckel[3]

[1]Interdisziplinäres Zentrum für Bioinformatik, Universität Leipzig, 04103 Leipzig
[2]Institut für Informatik, Universität Leipzig, 04109 Leipzig
[3]Universitätsfrauenklinik Leipzig, 04103 Leipzig
[4]Institut für Pathologie, Universität Leipzig, 04103 Leipzig
Email: braumann@izbi.uni-leipzig.de

Abstract. The analysis of the 3D structure of tumour invasion fronts within the uterine cervix is considered essential for both discovering and understanding inherent architectural-functional relationships. The variation range of the invasion patterns known so far reaches from a smooth tumour-host boundary to more diffusely spreading patterns, which all are supposed to have a different prognostic importance. However, any verbal morphological quantifications in previous studies have been made just on single histological sections. Therefore, the intention of this paper is twofold: to provide *reconstructed 3D tumoural tissue data* and to apply an *algorithmic tumour invasion quantification*. Thus, to stay as much as close to routine pathology we as well use HE-stained histological sections but as *serial sections* of remarkable extent (90–500 slices). Slicing and staining, however, may induce some severe artefacts rarely to avoid, mainly different kinds of distortions.
The paper introduces an extended processing chain doing a robust volume reconstruction starting from stacks of digitised transmitted light microscope colour images resulting in a 3D visualisation of the invasion front of the cervical tumour. For the invasion quantification we refer to *digital compactness* which is considered to be in tight correspondence to those invasion features pathologists generally are paying attention when verbally assessing 2D sections in routine.

1 Introduction

The main interest of our research is in the 3D characterisation of invasion patterns exhibited by squamous epithelial carcinoma of the uterine cervix. This is a current clinical question. By considering tissue volumes instead of single slices it is expected to enable new insight views about tumour morphology and growth, some of the present research fields in *tissue organisation*. In particular, a new quality of the structural and morphological assessment of the considered tumours is expected. At present, we focus on specimen out of regions around tumour invasion fronts. Properties of those fronts are supposed to have relevance for the further prognosis of the respective patient [1].

Fig. 1. An overview of the processing chain towards tumour invasion front quantification on 3D reconstructed histological serial sections. Solid items are briefly introduced.

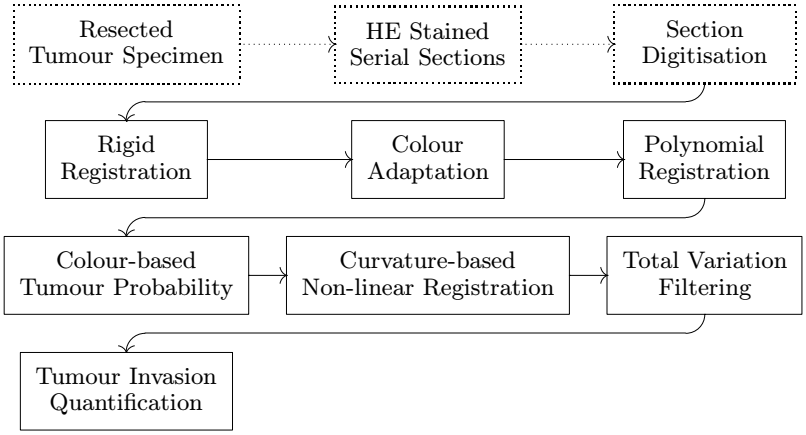

Unfortunately, at present there is no easy-to-apply direct 3D standard imaging technique available for obtaining details about those tumours. For our experimental investigations, despite its huge effort the method of choice for data acquisition was transmitted-light microscopy on stained histological serial sections. This setup inherently gives demand for both high level image processing and analysis. The paper mainly reports on the invasion quantification aspect of our ongoing research project aiming the further clarification of the morphological tumour expression.

2 Material and Methods

The processing chain given here (see fig. 1) is an extension of previous work [2]. Modifications and add-ons mainly consider the postprossing of the segmentation and the tumour invasion front quantification itself. While the latter is given in detail, all other steps regarding the 3D reconstruction and its key aspects are mentioned in brief.

Parameters of the Serial Sections

Sections typically have a rough extent of $2.5\,\mathrm{cm} \times 1.0\,\mathrm{cm}$. The raw digitisation area is 1300×1030 pixels corresponding to $10.45\,\mathrm{mm} \times 8.28\,\mathrm{mm} = 0.865\,\mathrm{cm}^2$ at a nominal pixel size of $8.04^2\,\mu\mathrm{m}^2$. The digitisation of the serial sections was carried out manually using a digital camera mounted on a transmitted light microscope. Under these conditions, due to the still limited field of view the digitisation practically should be considered as a rough selection of a region of interest (ROI) out of the tumour invasion front.

Rigid Registration

In the first stage, a serial section undergoes a successive pair-wise rigid co-registration of all slices using computed gray-levelled images (luminance of the

original colour images). By this, the data set is restricted to an effectively captured volume of interest (VOI). The approach we are using is a non-iterative two-step algorithm consisting of a combination of the polar-logarithmic Fourier-Mellin invariant (FMI, [3]) and phase-only matched filtering (POMF, [4]).

Colour Adaptation

Here we are going to treat fluctuations of the HE colour staining appearing along the serial sections in order to improve the tumour segmentation accomplished later on. The idea behind this simple but effective procedure is as follows: the concerned sample image's colour is subsequently adapted using a colour transform based on statistical distribution parameters determined referring to a certain reference image. Its essence is just to force all sample images to have the same mean and covariance matrix applying a linear transform.

Non-Linear Polynomial Registration

This third stage basically does the compensation for slice-global distortions applying a polynomial warping [5] using sparsely-populated displacement vector fields. Those displacement vectors rely on the pairwise correlate of partially overlapping image tiles (i. e. subimages). Again, we use POMF for their computation. For the estimates for the coefficients of the applied 5th degree polynomials, a multivariate linear regression using a least-squares error minimisation is accomplished.

Colour-based Tumour Probability

To treat the remainig local registration errors, we will need to subsequently apply yet another registration step. Instead of referring to some luminance related images, we are going to use scalar images highlighting the tumour regions. Those are generated simply by computing colour-based tumour probability maps relying on the HE staining, necessarily required for thresholding in tumour segmentation applied later on. The reason for swapping these two steps is to further attenuate artefacts which mostly occur outside the tumour regions which facilitates the final registration step. After manually obtaining representative tumour colour sample segments, we can estimate the multivariate distribution densities for both tumour and background (normal tissue, vessels, inflammation). The densities are estimated utilising chromaticities. What is taken as tumour probability is the quotient of the density for tumour and the sum of the densities for tumour and background.

Curvature-based Non-linear Registration

Now, what is necessary to remove local registration errors is the determination of the complete remaining displacement vector field. Therefore, a curvature-based non-linear registration described by a 4th order partial differential equation (PDE) is accomplished [6]. The coupled system of PDEs for the displacement fields is solved using successive approximation and discrete Fourier transform (DFT). The respective slice will undergo a spatial transformation according to the determined field.

Total Variation Filtering

Due to the pixel based colour segmentation the data contains a significant amount of noise. To selectively remove this noise component, but at the same

time to effectively keep edges a nonlinear total variation (TV) filter for the 3D data is used. Contrasting to e. g. nonlinear diffusion filtering, the advantage of TV filtering is to exhibit a fixed point representing the denoised image itself. The most important filtering parameter is the variance of the assumed Gaussian white noise. A solution method with low memory demands was proposed by Osher et. al. [7], basically transforming the energy minimisation into a time depend problem.

Tumour Invasion Quantification

Actual goal of the overall processing chain is to quantify the tumour invasion front. We apply a method relying on the sizes of both tumour surface and volume. A pretty much known description consisting of just these two components is *compactness*. This is an intrisic 3D object property and is dimensionless defined as ratio surface^3/volume^2 with the sphere as that particular object providing the absolute minimum at 36π. Direct compactness implementations, however, do lack of sufficient robustness, in the presence of noise surface enlargements would cause quite misleading compactness results. An alternative way to determine a compactness which far less can be irritated is *digital compactness* introduced for volumes in [8]. Instead of directly considering both surface and volume, digital compactness C_D relies on internal voxel contact surfaces and is defined simply as:

$$C_D = \frac{A_C - A_{C_{\min}}}{A_{C_{\max}} - A_{C_{\min}}}. \tag{1}$$

Herein, A_C denotes the number of contact surfaces within a 3D object consisting of n voxels, whereas correspondingly $A_{C_{\max}} = 3(n - n^{\frac{2}{3}})$ is the theoretical maximum of contact surfaces achieved with a cubic object consisting of the same n voxels (isotropic case). Constrasting to [8], we define $A_{C_{\min}} = 0$, in order to consistently allow for objects consisting of neighbouring voxels even without contact surfaces, so that $C_{D_{\max}} = 1$ for a "cube" and $C_{D_{\min}} = 0$ for a diagonal "voxel chain". A sphere, however, build up from discrete voxels, obviously would be evaluated little less compact than a cube.

3 Results and Discussion

The procedure meanwhile was applied to an overall of 13 specimens of squamous cell carcinoma of the uterine cervix with volumes in between $6.43\,\text{mm} \times 4.82\,\text{mm} \times 0.54\,\text{mm} = 16.74\,\text{mm}^3$ and $9.04\,\text{mm} \times 5.43\,\text{mm} \times 3.0\,\text{mm} = 147.26\,\text{mm}^3$. The compactnesses for all specimen are rather equally distributed between 0.883 (diffuse invasion) and 0.976 (close invasion, see fig. 2). A corresponding linear regression with a three-tiered 2D based clinical routine assessment based on single slices out of the same specimen yielded a correlation coefficient of 0.73.

With the above drafted scheme an objective quantification of the invasion of these tumours could be achieved for the first time. The obtained correlation indicates no complete conformity of the 3D compactness and the 2D verbal experts' assessment. Basically, this is plausible at all, since the basic motivation for doing this work was to provide the pathologist an additional but reliable means

Fig. 2. Views at three selected 3D reconstructed specimen with tumour invasion fronts, displayed as three-plane orthogonal reconstructions and surface renderings of segmented tumours. Individual digital compactnesses C_D are given below.

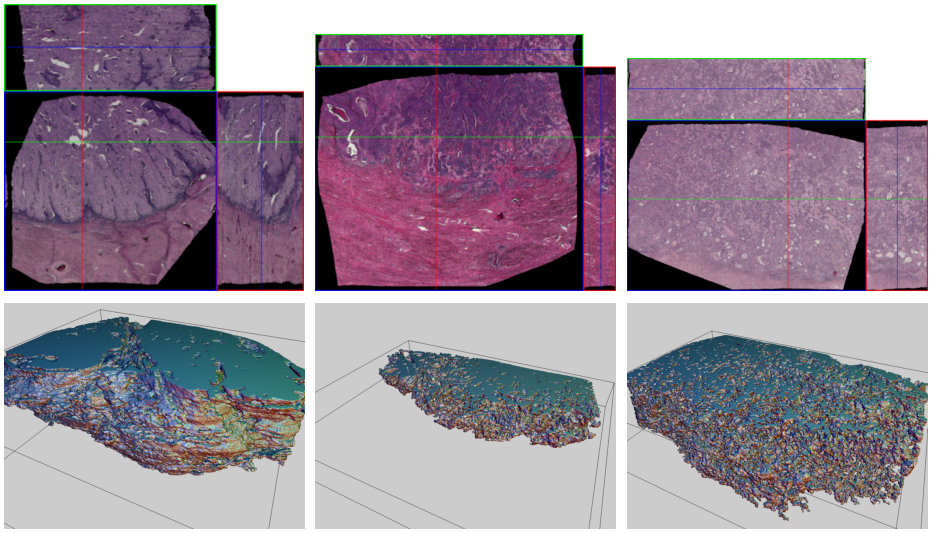

(a) 0.976 (b) 0.943 (c) 0.915

for an automated and by this objective 3D tumour assessment which obviously per se is considered superior of any verbal tumour invasion front description. From this point of view, the above mentioned correlation coefficient emphasises the appropriateness of the digital compactness as description method for the tumour invasion.

References

1. Horn LC, Fischer U, Bilek K: Morphologic Factors associated with Prognosis in Surgically Treated Cervical Cancer. Zentralbl Gynakol, 123(5):266–274, 2001.
2. Braumann UD, Kuska, JP, Einenkel, J: Dreidimensionale Rekonstruktion der Invasionsfront von Gebärmutterhalskarzinomen. Procs BVM 2003:230–234, Springer, 2003.
3. Casasent D, Psaltis D: Position, Rotation and Scale-Invariant Optical Correlation. Appl Opt 15(7):1795–1799, 1976.
4. Horner JL, Gianino PD: Phase-Only Matched Filtering. Appl Opt 23(6):812–816, 1984.
5. Hall EL: Computer Image Processing and Recognition. Academic Press, 1979.
6. Modersitzki J, Schmitt O, Fischer B: Effiziente, nicht-lineare Registrierung eines histologischen Serienschnittes durch das menschliche Gehirn. Procs BVM 2001:179–183, 2001.
7. Chan TF, Osher S, Shen J: The Digital TV Filter and Nonlinear Denoising. IEEE Trans Image Process 10(2):231-241, 2001
8. Bribiesca E: A Measure of Compactness for 3D Shapes. Comp Math Appl, 40(10-11):1275-1284, 2000.